Structure-Based Design of a Sulfonamide Probe for Fluorescence Anisotropy Detection of Zinc with a Carbonic Anhydrase-Based Biosensor

Daniel Elbaum,[†,§] Satish K. Nair,[†,||] Marcia W. Patchan,[‡] Richard B. Thompson,*[,‡] and David W. Christianson*[,†]

Contribution from the Department of Chemistry, University of Pennsylvania, Philadelphia, Pennsylvania 19104-6323, and Department of Biochemistry and Molecular Biology, University of Maryland School of Medicine, 108 N. Greene Street, Baltimore, Maryland 21201

Received December 6, 1995[⊗]

Abstract: Given the avid and selective metal binding properties of naturally-occurring metalloproteins, it is possible to exploit these systems in the development of novel sensors, i.e., "biosensors", for the detection of trace quantities of metal ions. Here, we exploit the high affinity of human carbonic anhydrase II (CAII) for zinc in the detection of nanomolar concentrations of this metal ion by fluorescence anisotropy using a fluorescein-derivatized arylsulfonamide probe, 4-aminosulfonyl[1-(4-*N*-(5-fluoresceinylthioureido)butyl)]benzamide (**3**). This probe was designed through an iterative, structure-based approach and was demonstrated to bind tightly only to the zinc-bound holoenzyme (K_d = 2.3 nM) and not the metal-free apoenzyme. Furthermore, the probe exhibits anisotropy that is proportional to the concentration of bound zinc, and this behavior can be exploited in the detection of zinc in the 10−1000 nM range. Strategies for the structure-based design of improved CAII-based metal ion biosensors are considered in view of these results.

Sensors based upon biological macromolecules are increasingly used for the selective detection of numerous chemical entities, including the detection of trace quantities (i.e., nanomolar concentrations) of metal ions. In particular, the advantages of metalloprotein-based biosensors over classical fluorometric chemical indicators for such applications include greater recognition and affinity for the target metal ion, discrimination among transition metals, and kinetically rapid sensor−analyte association and dissociation. Recently, Thompson and Jones[1] have exploited the avid and selective recognition of zinc by the metalloenzyme carbonic anhydrase in the design of an enzyme-based zinc biosensor. The basis of this sensor is the association of the zinc holoenzyme with the inhibitor 5-(dimethylamino)-1-naphthalenesulfonamide (dansylamide (**1**), K_d = 0.93 μM;[2] Figure 1), leading to a titratable change in the fluorescence emission wavelength and intensity.[3] Nanomolar concentrations of zinc can be detected and quantified by ratiometric methods by measuring the emission of free dansylamide at 580 nm and the emission of bound dansylamide at 470 nm when excited by 326 nm light, or by changes in the apparent fluorescence lifetime as the fraction of holoenzyme and thus bound dansylamide changes.[4]

The structure of human carbonic anhydrase II (CAII), determined and refined to 1.54 Å resolution,[5−7] reveals that the catalytically-required zinc ion resides at the base of a 15 Å deep cleft in the holoenzyme. Residues His-94, His-96, and His-119 coordinate to zinc, and the catalytically-active nucleophile, hydroxide ion, completes a tetrahedral metal coordination polyhedron. Zinc-bound hydroxide donates a hydrogen bond to the hydroxyl group of Thr-199, which in turn donates a hydrogen bond to Glu-106.[5−7] The binding of sulfonamide inhibitors such as dansylamide displaces zinc-bound hydroxide and maintains the tetrahedral metal coordination polyhedron,[8−12]

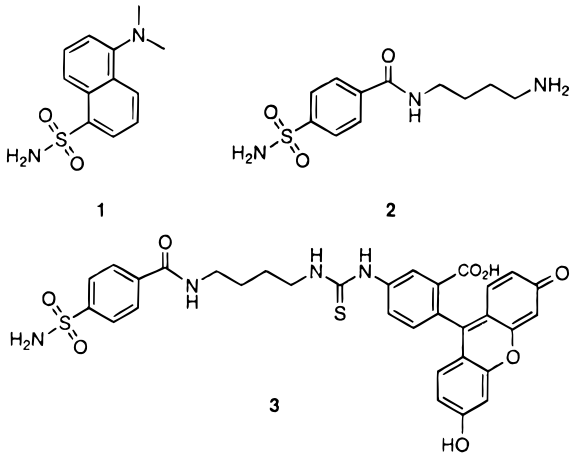

Figure 1. Chemical structures of 5-(dimethylamino)naphthalene-1-sulfonamide (dansylamide), **1**; 4-aminosulfonyl[1-(4-aminobutyl)]benzamide, **2**; and 4-aminosulfonyl[1-(4-*N*-(fluoresceinylthioureido)butyl)]-benzamide, **3**.

* To whom correspondence should be addressed.
† University of Pennsylvania.
‡ University of Maryland School of Medicine.
§ Current address: Vertex Pharmaceuticals, Inc., 40 Allston St., Cambridge, MA 02139.
|| Current address: Laboratories of Molecular Biophysics, The Rockefeller University, New York, NY 10021.
⊗ Abstract published in *Advance ACS Abstracts,* August 15, 1996.

(1) Thompson, R. B.; Jones, E. R. *Anal. Chem.* **1993**, *65*, 730−734.
(2) Nair, S. K.; Krebs, J. F.; Christianson, D. W.; Fierke, C. A. *Biochemistry* **1995**, *34*, 3981−3989.
(3) Chen, R. F.; Kernohan, J. C. *J. Biol. Chem.* **1967**, *242*, 5813−5823.
(4) Thompson, R. B.; Patchan, M. W. *J. Fluoresc.* **1995**, *5*, 123−130.
(5) Eriksson, A. E.; Jones, T. A.; Liljas, A. In *Zinc Enzymes*; Bertini, I., Luchinat, C., Maret, W., Zeppezauer, M., Eds.; Birkhauser: Boston, 1986; pp 317−328.
(6) Eriksson, A. E.; Jones, T. A.; Liljas, A. *Proteins: Struct. Funct. Genet.* **1988**, *4*, 274−282.
(7) Håkansson, K.; Carlsson, M.; Svensson, L. A.; Liljas, A. *J. Mol. Biol.* **1992**, *227*, 1192−1204.
(8) Eriksson, A. E.; Kylsten, P. M.; Jones, T. A.; Liljas, A. *Proteins: Struct. Funct. Gen.* **1988**, *4*, 283−293.
(9) Vidgren, J.; Liljas, A.; Walker, N. P. C. *Int. J. Biol. Macromol.* **1990**, *12*, 342−344.

S0002-7863(95)04102-3 CCC: $12.00

and an ionized sulfonamide nitrogen donates a hydrogen bond to Thr-199. Importantly, sulfonamides tightly bind only to the zinc holoenzyme and not to the metal-free apoenzyme. This property clearly facilitates the use of sulfonamide fluorophores to measure zinc binding to a CAII-based biosensor.[1]

Here we report the first-generation design of a CAII-based biosensor transducer which quantitates aqueous zinc concentrations by measuring fluorescence anisotropy of a fluorescein-based arylsulfonamide probe. In contrast to the dansylamide based biosensor,[1] which relies upon zinc-dependent changes in the wavelength and intensity of the fluorescence emission, the new detection scheme reported in the current work exploits the change in anisotropy of the fluorophore between the free and enzyme-bound states. Since the fluorophore only binds effectively to the zinc holoenzyme, the anisotropy change is proportional to the concentration of zinc holoenzyme, which in turn is proportional to the concentration of zinc in solution. Design of the fluorophore has been achieved by an iterative structure-based procedure in which the X-ray crystal structure of the CAII-arylsulfonamide **2** complex was determined and analyzed for the optimal attachment point for fluorescein (Figure 1); the design of **2** was based on inspection of the X-ray crystal structure of the complex between CAII and 4-((glycyltriethylene glycoloyl)carboxy)benzenesulfonamide.[11] Fluorophore **3** was then synthesized, its solution properties were evaluated including preliminary CAII-based zinc sensing, and the structure of its complex with CAII was determined by X-ray crystallographic methods.

Experimental Section

General Experimental Procedures. All reactions were performed in flame- or oven-dried glassware under a positive pressure of nitrogen. Air- and moisture-sensitive reagents were introduced *via* syringe or cannula through a rubber septum.

Physical Data. Melting points were measured with a Uni-Melt™ apparatus and were uncorrected. Infrared spectra (IR) were recorded using a Perkin-Elmer 1600 FT-IR spectrometer (ν max in cm^{-1}). Samples were prepared as KBr pellets. ^{1}H NMR spectra were recorded on a Bruker AM-500 (500 MHz) spectrometer at ambient temperature. Data were reported as follows: chemical shift in ppm using residual protic solvent as internal standard (1.93 for CD_3CN, and 2.49 for d_6-DMSO), multiplicity (br = broad, s = singlet, d = doublet, t = triplet, q = quartet, m = multiplet), coupling constant(s) in hertz, and integration. ^{13}C NMR were recorded on a Bruker AM-500 (125 MHz) spectrometer and were reported in ppm using solvent resonance as internal standard (39.5 for d_6-DMSO). All ^{13}C spectra were determined with complete proton decoupling. Mass spectra were obtained using a VG model ZAG-E mass spectrometer. Ultraviolet spectra (UV) were determined using an LKB 4054 spectrophotometer (λ max in nm). Fluorescence spectra were recorded on a Perkin-Elmer MFP-1 fluorescence spectrophotometer.

Chromatography. Analytical thin layer chromatography (TLC) was performed using either EM reagent 0.25 mm silica gel 60-F or EM reagent 0.25 mm RP-18 F_{254}s plates. Components were visualized with ultraviolet light (254 or 366 nm) and by staining with either ceric ammonium molybdate in 10% sulfuric acid or potassium permanganate in water. Ion exchange chromatography was performed using Dowex 50X8 200 mesh ion exchange resin (HCl form). Reverse-phase high-performance liquid chromatography (RP-HPLC) was performed using a Rainin HPLC system equipped with a Dynamax −60A C18 column (2.15 × 25 cm).

Solvents and Reagents. Dimethylformamide was distilled and stored over 4 Å molecular sieves prior to use. Acetonitrile (Gold label, Sure Seal® bottle) was purchased from the Aldrich Chemical Co. and used as received. Triethylamine was distilled from CaH_2 prior to use. Fluorescein-5-isothiocyanate was purchased from Molecular Probes and used without further purification.

4-Aminosulfonyl[1-(4-aminobutyl)]benzamide (2). The *N*-hydroxy succinimide ester of *p*-carboxybenzenesulfonamide (3.0 g, 10.06 mmol, 1 equiv) was dissolved in 33 mL of acetonitrile. Triethylamine (2.1 mL, 15.09 mmol, 1.5 equiv) and 1,4-diaminobutane (1.1 mL, 11.07 mmol, 1.1 equiv) were dissolved in 33 mL of acetonitrile in a separate flask. The latter solution was added via cannula to the first with vigorous stirring, and a white precipitate was observed. The suspension was stirred for 18 h after which the solvent was removed at reduced pressure. The crude white solid was purified by cation exchange chromatography over Dowex 50X8 200 mesh beads. Pure product was eluted with aqueous NH_4OH. Lyophilization yields 1.7 g (63%) of the product as a fine white solid: mp 130 °C dec; ^{1}H NMR (500 MHz, DMSO-d_6) δ 8.63 (bd, J = 33 Hz, 1H), 7.965 (d, J = 8.4 Hz, 2H), 7.87 (d, J = 8.4 Hz, 2H), 6.63 (s, 1H), 3.3 (s, 2H), 3.25 (m overlapping, 2H), 2.94 (bd, J = 5.9 Hz, 1H), 2.58 (t, J = 6.7 Hz, 1H), 1.56 (m, 2H), 1.43 (m, 2H); ^{13}C NMR (125 MHz, DMSO-d_6) δ 164.9, 157.2, 146.0, 137.5, 127.7, 125.5, 27.1, 26.4, 26.3; IR (KBr) 3297, 3064, 3031, 2973, 2932, 2874, 1738, 1649, 1517, 1453, 1391, 1366, 1244, 1167, 1109, 1052, 1029, 995, 906, 852, 752, 698, 667 cm^{-1}; MS (CI) *m/e* calcd for $C_{11}H_{18}N_3O_3S$ 272.1069, found 272.1078; 272 ([M + H^+]$^+$), 242, 184; white solid.

4-Aminosulfonyl[1-(4-*N*-(5-fluoresceinylthioureido)butyl)]-benzamide (3). Fluorescein-5-isothiocyanate (176.6 mg, 0.45 mmol, 1.1 equiv) was added to aminosulfonamide **2** (111.8 mg, 0.41 mmol, 1 equiv), and triethylamine (86 μL, 0.62 mmol, 1.5 equiv) was dissolved in 4.1 mL of dry dimethylformamide. The reaction mixture was stirred in the dark for 4 h and quenched with 1 M NH_4OH. The solvent was then removed under reduced pressure and a crude orange gum was purified by RP-HPLC eluting with a gradient of 30−50% CH_3CN/H_2O. Removal of the solvent by freeze drying resulted in 155 mg (57%) of an orange solid: mp 164 °C dec; R_F 0.4 (40% CH_3CN/H_2O C-18 RP); ^{1}H NMR (500 MHz, CD_3CN) δ 8.40 (s, 1H), 8.08 (s, 1H), 7.91 (s, 4H), 7.67 (s, 1H), 7.25 (s, 1H), 7.12 (d, 8.2, 1H), 6.97 (bd, J = 4.9 Hz, 1H), 6.69 (d overlapping, J = 11.1 Hz, 2H), 6.69 (s overlapping, 2H), 6.56 (dd, J = 8.6, 2.4 Hz, 2H), 5.73 (bs, 2H), 3.62 (bs, 2H), 3.43 (q, J = 6.3 Hz, 2H), 1.7−1.65 (m, 4H); IR (KBr) 3421, 3075, 2920, 2845, 1604, 1542, 1459, 1379, 1313, 1200, 1170, 1115, 852, 608 cm^{-1}; UV−vis (H_2O) λ_{max} 495 nm; MS (FAB) *m/e* calcd for $C_{32}H_{28}N_4O_8S_2Na$ 683.1246, found 683.1271; 683 ([M + Na^+]$^+$), 413, 391; orange solid.

Dissociation Constant. A solution of **3** (3×10^{-8} M) was prepared in 100 mM Tris−SO_4 (pH 8.0 at 24 °C). CAII holoenzyme was purchased from Sigma and used without further purification and was serially diluted with the stock solution of fluorophore. The anisotropy was determined at each concentration in triplicate (Figure 2). The following four equations were used to develop a description of the binding:

$$K_d = [\text{CAII}][\mathbf{3}]/[\text{CAII}\cdot\mathbf{3}] \quad (1)$$

$$[\text{CAII}]_t = [\text{CAII}] + [\text{CAII}\cdot\mathbf{3}] \quad (2)$$

$$[\mathbf{3}]_t = [\mathbf{3}] + [\text{CAII}\cdot\mathbf{3}] \quad (3)$$

$$r_o = f_b r_b + f_f r_f \quad (4)$$

Rearranging these equations to express the observed fluorescence anisotropy (r_o) in terms of the anisotropies of **3** when free (r_f) and bound (r_b) and the total concentrations of CAII and **3** yields:

$$r_o - r_f = (r_b - r_f)\{[([\mathbf{3}]_t + [\text{CAII}]_t + K_d) - \{([\mathbf{3}]_t + [\text{CAII}]_t + K_d)^2 - 4[\mathbf{3}]_t[\text{CAII}]_t\}^{1/2}]/2[\mathbf{3}]_t\} \quad (5)$$

where [CAII] and $[\text{CAII}]_t$ = concentration of free and total carbonic anhydrase II, respectively, [**3**] and $[\mathbf{3}]_t$ = concentration of free and total fluorophore **3**, respectively, [CAII·**3**] = concentration of the complex, f_b, f_f = fraction of bound and free fluorophore, respectively, and r_b, r_f

(10) Bunn, A. M. C.; Alexander, R. S.; Christianson, D. W. *J. Am. Chem. Soc.* **1994**, *116*, 5063−5068.
(11) Boriack, P. A.; Kingery-Wood, J.; Whitesides, G. M.; Christianson, D. W. *J. Med. Chem.* **1995**, *38*, 2286−2291.
(12) Nair, S. K.; Elbaum, D.; Christianson, D. W. *J. Biol. Chem.* **1996**, *271*, 1003−1007.

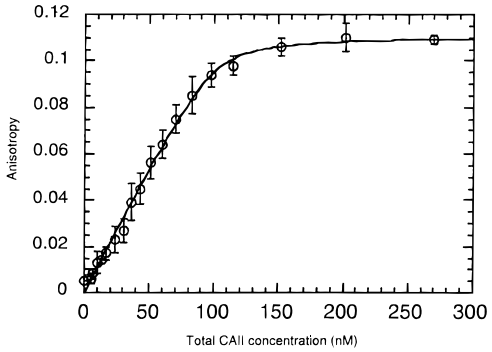

Figure 2. Anisotropy of 30 nM **3** as a function of the total concentration of CAII holoenzyme; the data were fit to eq 5 using the graphical program Kaleidagraph (Synergy Software, Reading, PA). Anisotropy $= (I_{||} - I_{\perp})/(I_{||} + 2I_{\perp})$; see eq 6. The curve demonstrates saturation binding with a dissociation constant of 2.3 ± 1.0 nM.

= the anisotropy of the bound and free fluorophore, respectively, where the unitless quantity *r*, anisotropy, is defined as:

$$r = (I_{||} - I_{\perp})/(I_{||} + 2I_{\perp}) \quad (6)$$

($I_{||}$ and $I_{\perp}$ are the intensity of the emission parallel and perpendicular to the excitation polarization, respectively.)

Thus, fitting the anisotropies measured as a function of the total concentration of CAII to eq 5 yields the K_d for the inhibitor. The curve fitting was performed with the program KaleidaGraph (Synergy Software, Reading, PA).

Detection of Zinc. Fluorescence anisotropies were measured on an SLM 8000c steady state fluorometer with a xenon lamp for excitation. Excitation was at 488 nm; emission was detected at 520 nm with a 4 nm bandpass on the monochromators and a KV500 filter on the emission channel. Blank spectra revealed negligible background fluorescence and no apparent scattered excitation; under these conditions the accuracy and precision of anisotropy measurements is ±0.003 or better. For a two-state system the fraction of the fluorescent inhibitor **3** bound f_b is a simple function of the anisotropies of the free and bound states (r_f and r_b, respectively), the ratio of their quantum yields $R = (q_b/q_f)$, and the measured anisotropy *r* at some intermediate saturation:[13]

$$f_b = (r - r_f)/((r_b - r)R + (r - r_f)) \quad (7)$$

The apparent quantum yield of **3** changed negligibly upon binding to CAII ($1 \leq R \leq 1.04$). Recombinant wild-type CAII was a generous gift from Professor Carol Fierke of Duke University. Apo-CAII was prepared by a previously described modification[14] of the method of Hunt and co-workers.[15] Briefly, using an Amicon diaflow apparatus CAII is filtered against 50 mM dipicolinic acid, pH 7.0 (0.65 mL/min, 100 min), and then 5 mM Tris−sulfate, pH 7.5, followed by chromatography on a PD-10 column. The procedure was performed twice to ensure complete removal of the zinc ion from CAII. Atomic absorption spectrophotometry (Galbraith Laboratories, Knoxville, TN) confirmed that the residual zinc in apoenzyme samples was <2%.

Crystallography. Crystals of human CAII (Sigma) were grown by the sitting drop method. A 5-μL drop containing CAII in 50 mM Tris−HCl (pH 8.0 at 24 °C) and saturated methyl mercuric acetate was added to a 5-μL drop containing 1.75−2.5 M ammonium sulfate and 50 mM Tris−HCl (pH 8.0 at 24 °C) and equilibrated against 1 mL of the precipitant buffer in the reservoir. After 1−2 weeks suitable crystals were transferred to 4 M K_3PO_4 (pH 10 at 24 °C), and then into an identical buffer solution containing 10 mM **2**. Crystals were allowed to soak for 1−2 days and then mounted and sealed in 0.5-mm glass capillaries with a small portion of mother liquor. A complete X-ray diffraction data set to 2.2-Å resolution was collected from one crystal of the CAII−**2** complex at room temperature on an R-Axis IIc image plate detector using Cu Kα radiation generated by a Rigaku RU-200 HB rotating anode operating at 50 mV and 100 mA. Data frames of 2.0° oscillation about the spindle axis ϕ were collected, with exposure times of 15 min/frame, for a total angular rotation range of 90° about ϕ. Raw data frames were analyzed with the MOSFLM suite of programs.[16] These crystals were isomorphous with crystals of the native enzyme[6,7] and belonged to space group $P2_1$ with unit cell dimensions of $a = 42.7$ Å, $b = 41.7$ Å, $c = 73.0$ Å, and $\beta = 104.6°$ as determined by the Kabsch autoindexing algorithm.[17] Data were scaled and corrected for Lorentz and polarization effects using ROTOVATA, and replicate and symmetry related reflections were merged using AGROVATA from the CCP4 suite of programs;[18] relevant data collection statistics are recorded in Table 1.

To prepare the CAII−**3** complex, CAII crystals were soaked in 4 M K_3PO_4 (pH 10 at 24 °C), ~8 mM **3**, for 3 months. For crystallographic data collection the crystals were equilibrated in 30% glycerol (v/v)−4 M K_3PO_4 (pH 10 at 24 °C) for 1 h before being mounted on a rayon loop, which was then flash frozen at −180 °C.[19] A complete X-ray diffraction data set to 2.4-Å resolution was collected at −180 °C on an R-Axis IIc image plate detector using Cu Kα radiation generated by a Rigaku RU-200 HB rotating anode operating at 50 mV and 100 mA. Data frames of 3.0° oscillation about the spindle axis ϕ were collected, with exposure times of 15 min/frame, for a total angular rotation range of 120° about ϕ. Data were processed as described for the CAII−**2** complex and relevant data collection statistics are recorded in Table 1.

Structure refinement was carried out using the simulated annealing method of Brünger and colleagues implemented in X-PLOR.[20] During the course of refinement, structure factors obtained from corrected

Table 1. Data Collection and Refinement Statistics for CAII−Inhibitor Complexes

	CAII−**2** complex	CAII−**3** complex
no. of crystals	1	1
no. of measd reflcns	49326	23619
no. of unique reflcns	13684	8797
multiplicity of unique reflcns	2.4	2.2
max resolution (Å)	2.2	2.4
overall completeness of data	99	88.5
completeness of data in the highest 0.1 Å resolution shell (%)	97	89
R_{merge}[a]	0.027	0.051
no. of water molecules in the final cycle of refinement	141	146
no. of reflcns used in refinement	12239	7637
R factor[b]	0.162	0.153
R_{free}[c]	0.217	0.268
rms deviation from ideal bond lengths (Å)	0.005	0.008
rms deviation from ideal bond angles (deg)	1.4	1.6
rms deviation from ideal dihedral angles (deg)	24.6	24.7
rms deviation from ideal improper dihedral angles (deg)	1.1	1.2

[a] R_{merge} for replicate reflections, $R = \sum|I_{hi} - \langle I_h\rangle|/\sum\langle I_h\rangle$; I_{hi} = intensity measured for reflection *h* in data set *i*, $\langle I_h\rangle$ = average intensity calculated for reflection *h* from replicate data. [b] Crystallographic *R* factor, $R = \sum||F_o| - |F_c||/\sum|F_o|$; $|F_o|$ and $|F_c|$ are the observed and calculated structure factors, respectively. [c] Free *R* factor, $R_{free} = \sum||F_o| - |F_c||/\sum|F_o|$, where $|F_o|$ and $|F_c|$ correspond to 1266 reflections excluded from refinement for the CAII−**2** complex, and 913 reflections excluded from refinement for the CAII−**3** complex.

(13) Lakowicz, J. R. In *Principles of Fluorescence Spectroscopy*; Plenum Press: New York, 1983; pp 112−187.
(14) Alexander, R. S.; Kiefer, L. L.; Fierke, C. A.; Christianson, D. W. *Biochemistry* **1993**, *32*, 1510−1518.
(15) Hunt, J. B.; Rhee, M.; Storm, C. B. *Anal. Biochem.* **1977**, *79*, 614−617.
(16) Nyborg, J.; Wonacott, A. J. In *The Rotation Method in Crystallography*; Arndt, U. W., Wonacott, A. J., Eds.; North-Holland: Amsterdam, 1977; pp 139−152.
(17) Kabsch, W. *Acta Crystallogr.* **1978**, *A32*, 922−923.
(18) Collaborative Computing Project, Number 4 *Acta Crystallogr.* **1994**, *D50*, 760−763.
(19) Hope, H. *Annu. Rev. Biophys. Biophys. Chem.* **1990**, *19*, 107−126.

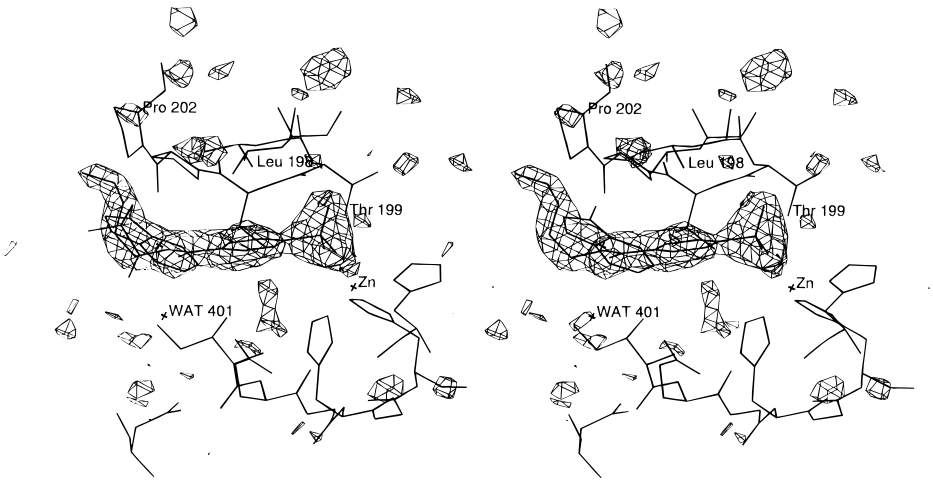

Figure 3. Omit electron density map of the CAII−**2** complex contoured at 2.5 σ. Enzyme residues Leu-198, Thr-199, Pro-202, Zn^{2+}, and water 401 are indicated. Water 302 (see text) is obscured by the inhibitor.

intensity data were used to generate difference electron density maps using Fourier coefficients $2|F_o| - |F_c|$ and $|F_o| - |F_c|$ with phases calculated from the in-progress model. Model building was performed with the graphic software CHAIN,[21] installed on a Silicon Graphics Indigo Workstation. Water molecules were fit into electron density peaks greater than 2.5σ if the peaks were within hydrogen bonding distance to a protein residue. Water molecules were removed from the model if their refined thermal *B*-factor was ≥ 50 Å^2. The appropriate inhibitor was modeled into each electron density map after the crystallographic *R* factor dropped below 0.19. Each refinement converged smoothly to crystallographic *R* factors of 0.162 and 0.153 for the CAII−**2** and CAII−**3** complexes, respectively, with excellent stereochemistry; relevant refinement statistics are recorded in Table 1. The rms coordinate error was estimated to be 0.15 and 0.27 Å for the CAII complex with **2** and **3**, respectively, using SIGMAA.[22] Final coordinates have been submitted to the Brookhaven Protein Data Bank.[23]

Results

Synthesis. Treatment of *p*-carboxybenzenesulfonamide with 1,4-diaminobutane in acetonitrile provided a white precipitate (**2**) subsequently purified by ion exchange chromatography. Addition of fluorescein-5-isothiocyanate to a solution of amine **2** in dimethylformamide yielded the expected compound **3** as an orange solid. Molecular structures of **2** and **3** are found in Figure 1.

Dissociation Constant of 3. The dissociation constant was determined by measuring the anisotropy of a 30 nM solution of fluorophore **3**, as a function of the total concentration of CAII (Figure 2). The fit of the observed data gives $K_d = 2.3 \pm 1.0$ nM. A Scatchard analysis of the fluorescence anisotropy data (not shown) demonstrates that the binding stoichiometry is 1:1, consistent with the crystallographic results (*vide infra*).

Detection of Zinc. In the presence of apo-CAII the fluorescence anisotropy of **3** is strongly dependent on the concentration of zinc ion, but in the absence of the apoprotein it is not (Figure 5). The slight increase in anisotropy observed at 1 nM Zn^{2+} when the apoprotein is added suggests that at the given protein and inhibitor concentrations a few percent of the inhibitor is bound; the binding of inhibitor is thus approximately 1000-fold weaker to the apoprotein than to the holoprotein. This is consistent with the fact that a significant portion of enzyme-inhibitor binding energy is derived from sulfonamide−zinc coordination. Loss of this interaction by zinc depletion results in a binding interaction which presumably relies on extensive hydrophobic contact between apoenzyme and inhibitor of a similar nature to that described by Boriack and colleagues.[11] Alternatively, some residual Zn^{2+} might be present in apoenzyme preparations, but atomic absorption analysis suggests that less than 2% of the protein in these preparations contains bound zinc.

At the relatively high concentrations used here (1 μM apoprotein, 1 μM inhibitor), binding of Zn^{2+} to the apoprotein and the inhibitor to the holoprotein is essentially stoichiometric due to their tight binding ($K_d = 4$ pM for zinc binding to the apoprotein,[24] and $K_d = 2.3$ nM for the inhibitor binding to the holoprotein, respectively); it would be awkward to measure the binding of Zn^{2+} to the wild type apoprotein at the commensurately low enzyme and inhibitor concentrations required to accurately determine the fractional saturation.[25] While the entire span of the titration curve is not depicted in Figure 5, it is evident that the fractional saturation of the enzyme with inhibitor, and thus with zinc, can be readily determined from the large change in anisotropy arising from inhibitor binding.

Crystal Structures. The three-dimensional structure of the CAII−**2** complex, determined at 2.2-Å resolution, shows that the overall structure of the protein remains largely unchanged upon inhibitor binding. The inhibitor binds in the active site of the enzyme as expected with the deprotonated sulfonamide displacing zinc-bound hydroxide as previously observed in other CAII−arylsulfonamide complexes.[8−11,26,27] An electron density map of the CAII−**2** complex is shown in Figure 3, and selected enzyme−inhibitor interactions are recorded in Table 2.

Despite the relative conformational freedom of the aliphatic tail of **2**, only one conformation of this tail is stabilized in the enzyme−inhibitor complex. Interestingly, the primary amino

(20) Brünger, A. T.; Kuriyan, J.; Karplus, M. *Science* **1987**, *235*, 458−460.
(21) Sack, J. S. *J. Mol. Graphics* **1988**, *6*, 224−225.
(22) Read, R. J. *Acta Crystallogr.* **1986**, *A42*, 140−149.
(23) Bernstein, F. C.; Koetzle, T. F.; Williams, G. J. B.; Meyer, E. F.; Brice, M. D.; Rodgers, J. R.; Kennard, O.; Shimanouchi, T.; Tasumi, M. *J. Mol. Biol.* **1977**, *112*, 535−542.
(24) Kiefer, L. L.; Krebs, J. F.; Paterno, S. A.; Fierke, C. A. *Biochemistry* **1993**, *32*, 9896−9900.
(25) Davenport, D. In *Fluorescence Spectroscopy: An Introduction for Biology and Medicine*; Pesce, A. J., Rosen, C.-G., Pasby, T. L., Eds.; Marcel Dekker: New York, 1971; pp 203−240.
(26) Baldwin, J. J.; Ponticello, G. S.; Anderson, P. S.; Christy, M. E.; Murcko, M. A.; Randall, W. C.; Schwam, H.; Sugrue, M. F.; Springer, J. P.; Gautheron, P.; Grove, J.; Mallorga, P.; Viader, M.; McKeever, B. M.; Navia, M. A. *J. Med. Chem.* **1989**, *32*, 2510−2513.
(27) Prugh, J. D.; Hartman, G. D.; Mallorga, P. J.; McKeever, B. M.; Michelson, S. R.; Murcko, M. A.; Schwam, H.; Smith, R. L.; Sondey, J. M.; Springer, J. P.; Sugrue, M. F. *J. Med. Chem.* **1991**, *34*, 1805−1818.

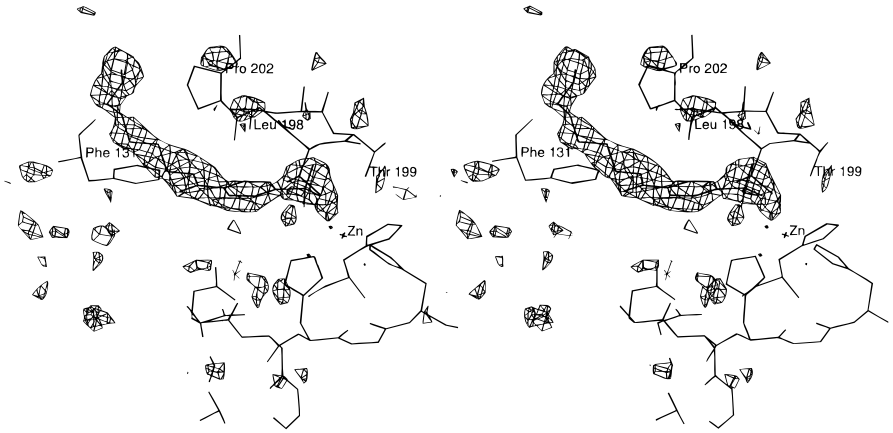

Figure 4. Omit electron density map of the CAII−**3** complex contoured at 2.4 σ. Enzyme residues Phe-131, Leu-198, Thr-199, Pro-202, and Zn^{2+} are indicated. Inhibitor density is complete out to the thiocarbonyl moiety. No electron density is observed for the fluorescein portion of compound **3**, which is indicative of molecular disorder.

Table 2. Selected CAII Inhibitor Interactions

inhibitor atom	enzyme residue	separation (Å) **2**	separation (Å) **3**
sulfonamide N1	Zn^{2+}	2.1	2.4
sulfonamide N1	Thr-199 Oγ	2.8[a]	3.1[a]
sulfonamide O1A	Thr-199 NH	3.1[a]	3.5
ring C2	Thr-200 Oγ	3.3	3.3
ring C3	Thr-200 Oγ	3.3	3.6
NH	H_2O 302	2.9[a]	
C═O	Phe-131 Cζ	3.3	2.9
C═O	H_2O 401	3.0[a]	

[a] Denotes a presumed hydrogen bond as judged from distance and stereochemical criteria.

group does not engage in any hydrogen bond contacts with the protein or with ordered solvent molecules. Thus, only hydrophobic interactions with Leu-198 and Pro-202 appear to stabilize the bound conformation of the aliphatic tail of **2**. The protein loses 69 Å^2 of solvent accessible surface on binding **2**. This is similar to the binding behavior of 4-((glycyltriethylene glycoloyl)carboxy)benzenesulfonamide: extensive hydrophobic interactions between the Pro-202/Leu-198 region stabilize the ethylene glycol-based tail of this inhibitor in a nearly identical conformation.[11]

In addition to the interactions discussed above, there are two water-mediated hydrogen bonds between CAII and **2**. The amide oxygen of **2** accepts a hydrogen bond from water 401, which in turn accepts a hydrogen bond from the side chain amide of Gln-92. Facing the opposite side of the active site cleft the amide NH of **2** donates a hydrogen bond to water 302, which in turn donates a hydrogen bond to the backbone carbonyl oxygen of Pro-201. These two interactions are identical to water-mediated hydrogen bonds observed in the complex of CAII with arylsulfonamide 4-((glycyltriethylene glycoloyl)-carboxy)benzenesulfonamide,[11] and these protein−solvent−inhibitor interactions presumably help to stabilize the binding conformation of the inhibitor aromatic ring.

The three-dimensional structure of the CAII−**3** complex, determined at 2.4-Å resolution, shows that the overall structure of the protein remains largely unchanged upon inhibitor binding. The arylsulfonamide portion of inhibitor **3** binds in the active site of the enzyme in a manner similar to that of **2**. However, the model indicates that the aliphatic tail is in a more extended conformation than seen in compound **2**. This extension positions the formerly terminal nitrogen beyond Pro-202 rather than next to it. Furthermore, the fluorescein moiety of **3** is not visible in the electron density map, so it is presumed to be disordered on the time scale required for X-ray diffraction data collection.

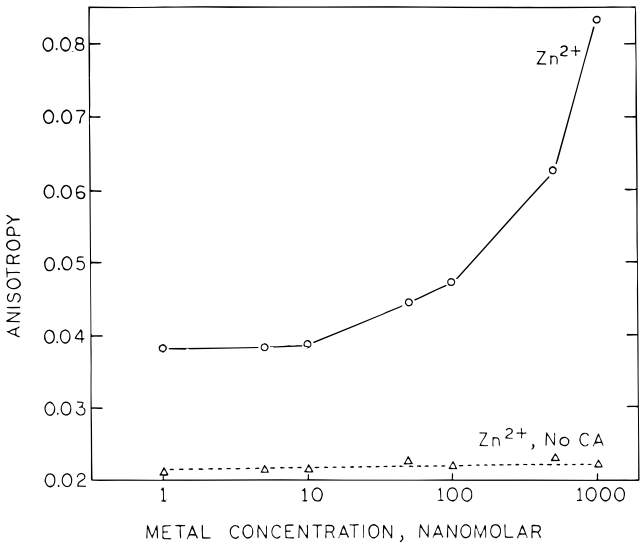

Figure 5. Zn^{2+} concentration-dependent fluorescence anisotropies of 1 μM **3** are depicted in the absence (triangles) and presence (circles) of 1 μM apo-CAII. Anisotropy = $(I_{||} - I_{\perp})/(I_{||} + 2I_{\perp})$; see eq 6.

An electron density map of the CAII−**3** complex is shown in Figure 4, and selected enzyme−inhibitor interactions are recorded in Table 2. We note that the hydrophobic and hydrogen bond interactions described in the previous paragraph are presumably sufficient to stabilize inhibitor binding to the apoenzyme, although with ∼10^3-fold weaker affinity, in the absence of sulfonamide−zinc coordination.

Discussion

Enzyme−Inhibitor Affinity Determinants in the CAII Active Site. That sulfonamide **3** binds to CAII with nanomolar affinity (K_d = 2.3 nM) is notable given that benzenesulfonamide, which lacks a *para*-substituted fluorophore "tail", binds to the enzyme with K_d = 1.54 μM.[28] The fluorophore tail group of **3** therefore contributes a factor of ∼10^3 to enzyme−inhibitor affinity, which is remarkable in view of the disorder of all but its aliphatic linker. Since the fluorescein moiety of **3** is disordered in the electron density map of the CAII−**3** complex (Figure 4), it cannot contribute substantially (probably no more than a factor of 10) to enzyme−inhibitor affinity. For example, different amino acids substituted at the termini of arylsulfonamide *para*-substituted ethylene glycol tail groups exert a subtle

(28) Taylor, P. W.; King, R. W.; Burgen, A. S. V. *Biochemistry* **1970**, *9*, 2638−2645.

effect (factors of 1−6) on enzyme−inhibitor affinity even though the amino acids are observed to be disordered in electron density maps.[11]

Therefore, assuming that the disordered fluorophore of **3** contributes a maximum of a factor of 10 to enzyme−inhibitor affinity, we estimate that the aliphatic tail of **3** alone contributes a factor of ∼100 to affinity. Inspection of the three-dimensional structure of the CAII−**3** complex suggests that the sole basis for this affinity enhancement is the loss of 69 Å^2 of solvent-exposed surface area on the protein in the enzyme−inhibitor complex. The aliphatic tail of **3** interacts extensively with the Pro-202/Leu-198 hydrophobic wall in the CAII active site; thus, this interaction appears to be the primary determinant of enhanced enzyme−inhibitor affinity, and this is consistent with structure-affinity measurements made for other *para*-substituted arylsulfonamide inhibitors.[10,11,29,30] In order to tune the affinity of second-generation fluorophore probes as they bind to CAII, interactions with the Pro-202/Leu-198 hydrophobic wall can be modulated accordingly.

CAII as the Zinc Biosensor Prototype. The ability to transduce the concentration of a metal ion such as Zn^{2+} as a change in fluorescence anisotropy has far-reaching implications for chemical analysis, and the experiments described herein provide an important first step for the development of CAII in such biosensor applications. Of course, fluorescence anisotropy and polarization measurements have long been used to quantitate the concentrations of small molecules such as drugs and hormones by the technique of fluorescence polarization immunoassay.[31] The widespread use of the method is attributable to the relatively good sensitivity, high accuracy and precision, simple instrumentation, and excellent freedom from artifact of the technique. We note that the instrumentation is significantly simpler and cheaper than that previously used in carbonic anhydrase-based biosensing of metals by fluorescence lifetime measurements.[4] However, to our knowledge fluorescence anisotropy has yet to be successfully measured through an optical fiber, so at this time the method does not appear suited for use with fiber optic sensors. Nevertheless, the prospect of handheld devices capable of determining metal ion concentrations with high selectivity in aqueous solution at part-per-billion levels in real time is clearly of interest for applications in environmental monitoring, industrial hygiene, and wastewater treatment.

In order to improve the sensitivity and response time of a CAII-based zinc biosensor in the 1−10 nM Zn^{2+} range, a combination of two approaches can be taken. The first approach focuses on the recognition molecule, in that the metal binding properties of CAII (protein−zinc affinity and equilibrium kinetics) can be engineered. CAII−zinc affinity can be improved or diminished by augmenting or altering the wild-type zinc ligands, respectively.[24,32−36] For example, by substituting cysteine or glutamate for Thr-199, the tetradentate protein−zinc coordination polyhedron exhibits enhanced affinity (K_d = 1.1 pM and 20 fM, respectively; wild type K_d = 4 pM).[24,33,36] In CAII biosensor applications these variants must be capable of binding a fluorescent probe molecule, and the addition of a fourth protein ligand to zinc would hinder sulfonamide binding. However, the fourth zinc ligand engineered at position 199 of these variants can be displaced by sulfonamide binding, as demonstrated in crystallographic studies of the Thr-199 → Cys variant.[24,33]

Additionally, "indirect" metal ligands (i.e., residues that accept hydrogen bonds from histidine zinc ligands) can be varied to modulate protein−zinc affinity and equilibrium kinetics.[37−39] Significantly, the modification of certain indirect zinc ligands in CAII results in the enhancement of zinc association and dissociation kinetics.[40] Thus, the response time and the recycling time of a CAII-based biosensor can be tuned specifically for the demands of a particular sensing task.

The second general approach for improving the CAII-based biosensor focuses on the optimization of the fluorophore probe, **3**. Since the observed maximum anisotropy is lower than anticipated (0.11 rather than 0.3), it is possible that the sensitivity of this assay may be improved by increasing the maximum anisotropy. The structural data on the CAII-**2** and CAII-**3** complexes reveal that the fluorophore of **3** resides just outside of the constricted, cone-shaped active site of the enzyme. Therefore, the fluorophore of **3** is capable of some degree of free rotation independent of the enzyme to which it is bound (consistent with its presumed disorder in the electron density map (Figure 4)), so the rotational correlation time of the fluorophore is not rigorously coupled to that of the enzyme. To strengthen the coupling of the rotational correlation time of the fluorophore with that of CAII, we propose to shorten the aliphatic linker between the fluorophore and the arylsulfonamide by 1−2 methylene units. This will draw the fluorophore deeper into the active site cleft upon binding of the arylsulfonamide to zinc, its rotational freedom will thus be reduced, and its maximum anisotropy will increase. The synthesis of appropriately redesigned arylsulfonamide fluorophores is currently underway, and these fluorophores will be evaluated with CAII variants exhibiting metal affinities and equilibrium kinetics optimized for zinc biosensor applications.

It is instructive to compare the potential of a CAII-based biosensor with sensors already in existence. To our knowledge the majority of sensors for metal ions are the "chemosensor" variety.[41,42] These sensors have signal transduction mechanisms based upon fluorescence intensity changes, either individual or ratiometric, or fluorescence lifetime changes of metallofluorescent indicators upon binding a metal ion. As these "chemosensors" are mainly of low molecular weight, fluorescence anisotropy is not a useful signal transduction method. Furthermore, these chemosensors usually have a functional range of detection in the μM to mM concentration of analyte. The CAII-based biosensor has high sensitivity, with a detection of nM to μM concentration of Zn^{2+}. Moreover, the metal equilibration kinetics, and therefore the response times, of the biosensor may be modulated in a systematic fashion.[37−39] Most notably, the use of a protein molecule as an analyte recognition element makes it possible to exploit fluorescence anisotropy for signal

(29) Jain, A.; Whitesides, G. M.; Alexander, R. S.; Christianson, D. W. *J. Med. Chem.* **1994**, *37*, 2100−2105.
(30) Gao, J.; Qiao, S.; Whitesides, G. M. *J. Med. Chem.* **1995**, *38*, 2292−2301.
(31) Barnard, G. *Prog. Clin. Biol. Res.* **1988**, *285*, 15−37.
(32) Kiefer, L. L.; Ippolito, J. A.; Fierke, C. A.; Christianson, D. W. *J. Am. Chem. Soc.* **1993**, *115*, 12581−12582.
(33) Ippolito, J. A.; Christianson, D. W. *Biochemistry* **1993**, *32*, 9901−9905.
(34) Kiefer, L. L.; Fierke, C. A. *Biochemistry* **1994**, *33*, 15233−15240.
(35) Ippolito, J. A.; Christianson, D. W. *Biochemistry* **1994**, *33*, 15241−15249.
(36) Ippolito, J. A.; Baird, T. T.; McGee, S. A.; Christianson, D. W.; Fierke, C. A. *Proc. Natl. Acad. Sci. U.S.A.* **1995**, *92*, 5017−5021.
(37) Lesburg, C. A.; Christianson, D. W. *J. Am. Chem. Soc.* **1995**, *117*, 6838−6844.
(38) Kiefer, L. L.; Paterno, S. A.; Fierke, C. A. *J. Am. Chem. Soc.* **1995**, *117*, 6831−6837.
(39) Christianson, D. W.; Alexander, R. S. *J. Am. Chem. Soc.* **1989**, *111*, 6412−6419.
(40) Huang, C.-C.; Lesburg, C. A.; Kiefer, L. L.; Fierke, C. A.; Christianson, D. W. *Biochemistry* **1996**, *35*, 3439−3446.
(41) *Fluorescent Chemosensors for Ion and Molecule Recognition*; Czarnik, A. W., Ed.; American Chemical Society: Washington, 1993.
(42) Czarnik, A. W. *Chem. Biol.* **1995**, *2*, 423−428.

transduction: this cannot be done with a small molecule-based sensor. This is the first demonstration that this technique can be used in the detection of nanomolar concentrations of Zn^{2+}, and further redesign of both the sulfonamide probe and the zinc binding site of CAII will lead to the optimization of this novel zinc biosensor.

Acknowledgment. This work was supported by grants from the Office of Naval Research to D.W.C. and R.B.T., and D.W.C. also thanks the Office of Naval Research for an equipment grant in support of the X-ray data acquisition facility. D.E. was supported in part by NIH Postdoctoral Fellowship F32 CA62613. We thank Drs. Darin S. Katz, Carol A. Fierke, and Jean Duhamel for helpful discussions. Finally, we thank Professors Ponzy Lu and Michael Therien for generous access to their fluorometers, and Professor Amos B. Smith for use of an HPLC.

JA954102E